2024 IEEE International Conference on Robotics and Automation (ICRA 2024)
May 13-17, 2024. Yokohama, Japan

Preliminary Study of Fingertip and Wrist Motion Based Haptic Controller for Robotically Assisted Micro- and Supermicrosurgery

Muneaki Miyasaka, Pepijn Van Esch, Atsushi Morikawa, and Kotaro Tadano

***Abstract*— One issue of robotic microsurgery is that compared to manual surgery, the operation time tends to be longer due to high motion scaling. To address this issue, we developed a new controller that can provide the accuracy required for microsurgery without a high scaling factor by utilizing fingertip and wrist motions. Also, for the better outcome of surgery, the proposed controller has a force feedback function which is not available for the existing controllers for microsurgical robots. A challenge of designing such a controller is associated with the size requirement. For conventional microsurgery, surgeons perform surgical procedures while looking at the eyepieces of a surgical microscope and the same applies for robotic microsurgery. The only space available to manipulate controllers is a narrow space between the patient/surgical bed and the surgeon. To satisfy this constraint, the proposed controller is integrated with a handrest and the controller's DOFs are strategically allocated. In this work, as the first step of addressing the issue of prolonged operational time, we built a prototype controller and evaluated the accuracy and task space with simulations. The results indicated that by using the fingertip and wrist motions with a scaling factor of 3x, 0.5 mm diameter circles could be traced with a mean bidirectional precision of 0.0485 mm. Also, 10.0 mm diameter circles were traceable with the same scaling factor.**

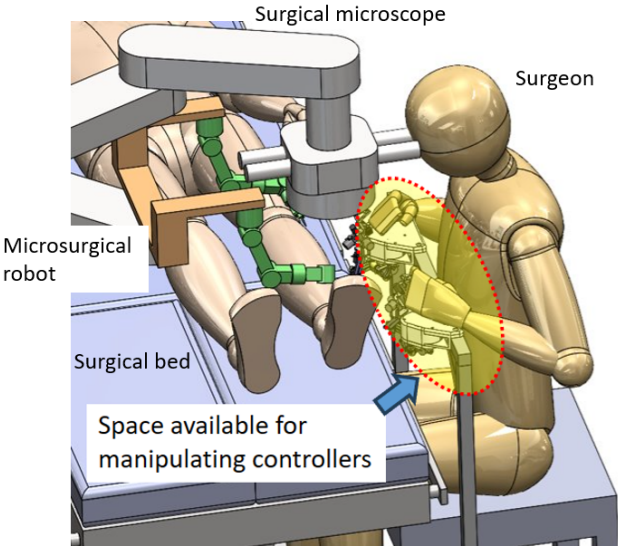

Fig. 1. Space available to manipulate controllers for robotically assisted microsurgery.

I. INTRODUCTION

Microsurgery is a type of surgery that involves with anastomosis of small blood vessels and nerves in a millimeter scale employed in the fields such as free flap reconstruction and nerve surgery. Anastomosis of even finer vessels between 0.3 and 0.8 mm, employed in lymphatic surgery, is called Supermicrosurgery. For micro- and supermicrosugery, precisions of 100 μm and 30 μm are required respectively. [1]–[3]. Supermicrosurgery is extremely technically demanding and even for experienced and skilled surgeons, the surgical performance is limited due to the precision and dexterity of the human hands [4], [5].

To break through the limitation of the human hand and make micro- or supermicrosurgery widely available, robotic systems specialized in small scale surgery have been introduced [1], [6], [7]. Although these robots permit the surgeon to perform fine scale surgeries with the aid of motion scaling and tremor filtration, studies have shown that the anastomotis times were longer for the robotic surgery compared with the manual surgery [8]–[10]. In the most recent clinical studies, motion scaling of up to 20x was implemented for lymphatic surgery. This study showed that higher motion scaling is a contributing factor to a prolonged operational time [9]–[11].

The conventional manual microsurgery is performed with manipulation of microsurgical tools held with fingertips. While surgeons are capable of performing fine submillimeter tasks, a few centimeter-range motion can also be made to cover the entire task space. For the current method of using the controllers with a high scaling factor, operators are required to move the controller in a large space with the arm more dominantly rather than the fingertips. If a controller could allow operators to utilize their fingertip motions, similar to conventional microsurgery, a lower scaling factor could be realized while still allowing a less demanding surgical skill as current controllers do. Through this, the operational time could become shorter and the difficulty of micro- and supermicrosurgery would be alleviated. While the precision and dexterity of the human hand/fingers are limited and there is a difference between the skills of different groups of surgeons, a scaling factor of less than 5x could be sufficient to meet both the motion accuracy and task space required for microsurgery. In addition, haptic feedback capability is preferred as it is missing for the existing robots, and it could potentially improve the surgery time and quality [10], [12], [13].

In the design of controllers for microsurgical robots, a unique constraint is the space usable for manoeuvring

Muneaki Miyasaka (m-miyasaka.rfc@riverfieldinc.com), Pepijn Van Esch (p-esch.rfc@riverfieldinc.com), and Atsushi Morikawa (a-morikawa.rfc@riverfieldinc.com) are with Riverfield inc., Japan and Kotaro Tadano (tadano.k.aa@m.titech.ac.jp / k-tadano.rfc@riverfieldinc.com) is with Laboratory for Future Interdisciplinary Research of Science and Technology, Tokyo Institute of Technology, Japan and with Riverfield inc., Japan

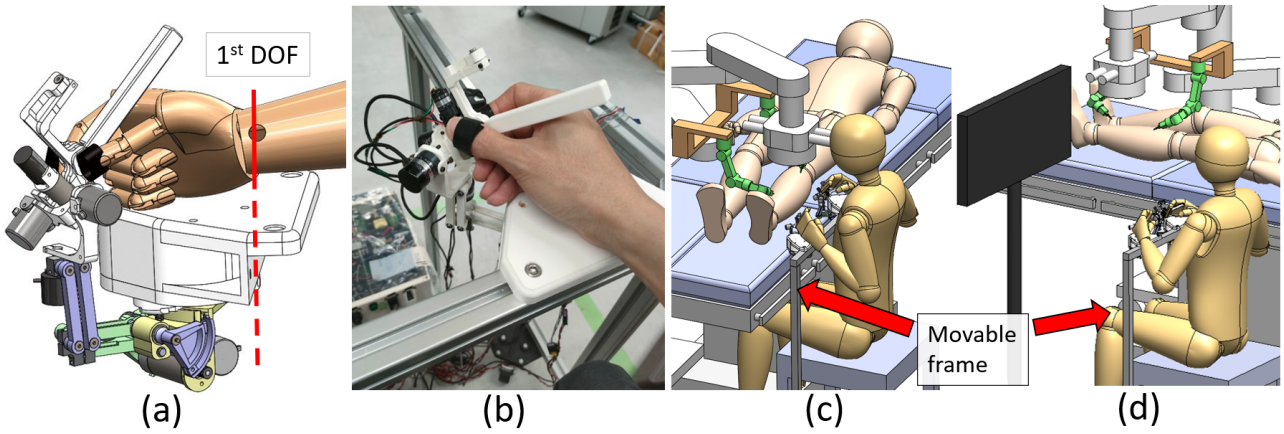

Fig. 2. (a)3D illustration and (b)prototype of the proposed controller. Setup of the controller when it is used with (c)a conventional surgical microscope and (d)surgical microscope with a heads-up monitor.

the controller. Because surgeons need to perform surgical procedures while looking at the eyepieces of the surgical microscope, only a narrow space between the patient/surgical bed and the surgeon is available (Fig.1). Although recent surgical microscopes provide heads up surgery by viewing the microscopic image on a panel display, such microscopes are not available for all the hospitals. Therefore, it is important to design a controller usable with the conventional surgical setup. The existing haptic controllers such as Touch, Phantom (3D Systems Inc), Omega.x, and Sigma.7 (Force Dimension) are not suitable for microsurgery as they do not meet the aforementioned requirement [14], [15]. The unique design of the proposed controller is that all the mechanisms are placed below the handrest. The translational part of the controller consists of one serial and two parallel linkages. By bringing the 1st degree of freedom (DOF) right underneath the hand, the proposed controller achieved sufficient workspace without interference with the surroundings and operator.

Our final goal is to shorten the surgical time for robotic microsurgery. As a preliminary study, the purpose of this research is to introduce a new haptic controller that 1. realizes both fine and large motions with a low scaling factor by utilizing the fingertip and wrist motions while stabilizing the hand on a handrest and 2. overcomes the spatial constraint by strategically placing the DOFs around a handrest. In this paper, we investigate if the proposed controller is capable of achieving the precision required for micro- and supermicrosurgery with a low scaling factor. We built a prototype controller and evaluated the level of precision that can be achieved in simulations. The organization of this paper is as follows. Section II explains the detailed design of the controller and Section III presents the experimental evaluation we conducted to investigate the performance of the prototype. In section IV and V, discussions and conclusions are stated.

II. System Description

For the design of the microsurgical controller, the below requirements are taken into account.

- The controller needs to fit between the surgical bed and the surgeon and there should be no interference between the hand/controller and the surrounding environment (i.e. patient, surgical bed, and surgical microscope.) while manoeuvring the controller.
- The controller needs to be separated from the surgical bed so it can be used for teleoperation in case a heads-up monitor is available.
- The mechanical impedance should be as low as possible to achieve fine finger motions with haptic feedback and to avoid operator's fatigue.
- The workspace of the controller should cover the operating volume of ϕ 20 $\times$ 20 mm and the suture handling volume of ϕ 30 $\times$ 30 mm after motion scaling [2].

The unique design element of the proposed controller is the placement of the controller's DOFs around the handrest. By bringing the first rotational DOF below the handrest along the rotational axis of the wrist, the range of motion of the fingertips caused by the wrist rotation is fully covered while keeping the mechanism compact. Besides, the handrest helps stabilize the operator's hand and contributes to the fine manipulation of the controller. There is no interference between the hand and the mechanism throughout the workspace. Since the controller is compact, it can be placed in a narrow space in front of the surgeon without interfering with the surgical bed (Fig. 2 (a, b)). Since the controller can be attached to a movable frame, it can be used both next to and away from the surgical bed. (Fig. 2 (c, d)).

The controller consists of four active (x, y, z translations and pinching) and three passive (yaw, pitch, and roll) DOFs. The translations, orientations, and pinching are provided by DOFs 1 to 3, 4 to 6, and 7 respectively (Fig. 3 (a)). The translational part consists of one serial and two parallel links. The parallel links were implemented for the DOFs 2 and 3 to keep the orientation of yaw, pitch, and roll independent of the translational motion within the workspace. In addition, the controller is equipped with two passive DOFs without encoders, DOF 8 at the index finger along the pinching axis, and DOF 9 at the thumb along the pitch axis. These passive

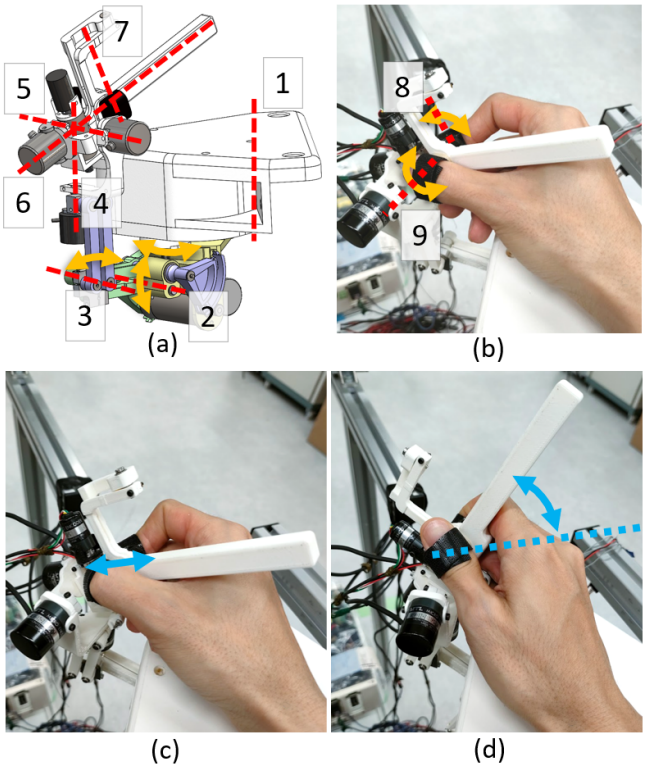

Fig. 3. (a)DOF arrangement of the proposed controller. DOFs 1 to 3, DOFs 4 to 6, and DOF 7 provide the 3D translation, orientation, and pinching motion respectively. (b)Two passive DOFs (DOFs 8 and 9) without encoders at the fingertips. Those passive DOFs provide (c)In-and-out motion and (d)pitch rotation only by using the finger motions without changing the hand position.

DOFs enable the in-and-out motion and pitch rotation by only using the fingertip movement without changing the hand position, which are also available for surgery with manual instruments (Fig. 3 (b-d)).

Because the size is compact, the linkages are small and have a low weight and inertia. This leads to low loads and friction at the joints. Also, the center of mass for yaw, pitch, and roll is designed to be nearby each axis to minimize the inertial effect. In other words, the mechanical impedance of the controller is low and it facilitates fine motions through the fingertips with minimal fatigue. In this prototype, the linkages were 3d printed from Ultimaker tough PLA.

The active DOFs are equipped with DCX-16L (DOF 1), DCX-22S (DOF 2,3), and DCX-16S (DOF 7) brushed DC motors (Maxon group, Switzerland). In addition to providing the gravity compensation, the translational DOFs are able to generate continuous feedback force up to 2.0 to 3.5 N. For pinching, the continuous feedback force is up to 3.5 N. DOFs 1 to 6 are equipped with either a build-in encoder with the motor or the MEH-12/MEA-14 encoder (Microtech Laboratory Inc., Japan) that can provide resolution of either 0.005 or 0.01°. The encoder for pinching is the MEH-9 (Microtech Laboratory Inc., Japan) with 0.36° resolution.

The position of the controller's tip (Px, Py, Pz) is calculated as follows.

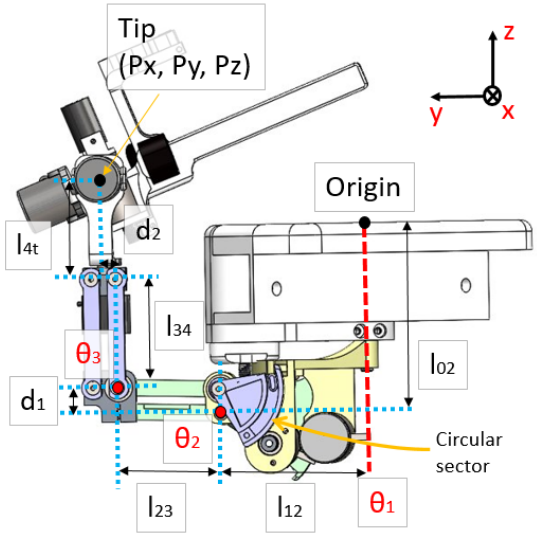

Fig. 4. Illustration of the controller's design parameters.

$$Px = (l_{12} + l_{23}\cos\theta_2 + l_{34}\sin\theta_3)\sin\theta_1 \quad (1)$$

$$Py = (l_{12} + l_{23}\cos\theta_2 + l_{34}\sin\theta_3 + d_2)\cos\theta_1 \quad (2)$$

$$Pz = -l_{02} - l_{23}\sin\theta_2 + d_1 + l_{34}\cos\theta_3 + l_{4t} \quad (3)$$

where all the design parameters are indicated in Fig. 4.

In Fig. 5, the workspace of the tip of the controller is plotted. Here it is shown that the prototype is able to cover a space of roughly 90W x 40H x 50D mm. The range of the yaw, pitch, and roll motions are ± 90°, 0-70°, and ±70° respectively.

III. Experimental Evaluation

A. Setup

To evaluate the capability of the controller to perform both fine and large motions with a single low scaling factor, we asked 10 novice participants (31.7±5.4 years old, right handed males) to perform four experiments using their dominant hand while sitting on a chair comfortably. Each experiment consists of following a circular trajectory with different combinations of the diameter, width, and plane in which the circle is displayed (Table I). As the depth perception is difficult in the simulations, the circles for both x-y and y-z plane experiments are displayed such that the circles are visible on a 2D plane (i.e. in-out finger motion controls the up-down motion of the pointer for the x-y plane experiments). The circles for the experiments A and C represent the scaling of supermicrosurgery and the experiments B and D are to demonstrate the large movements which do not require fine motions.

The participants were asked to trace the circle by controlling the white pointer with the controller. The color of the ring turns from red to blue when the pointer is within the ring. When the pointer touches the large yellow circle, the yellow circle shifts counter clockwise within the ring (Fig. 6). After tracing one full circle, the next circle appears. The

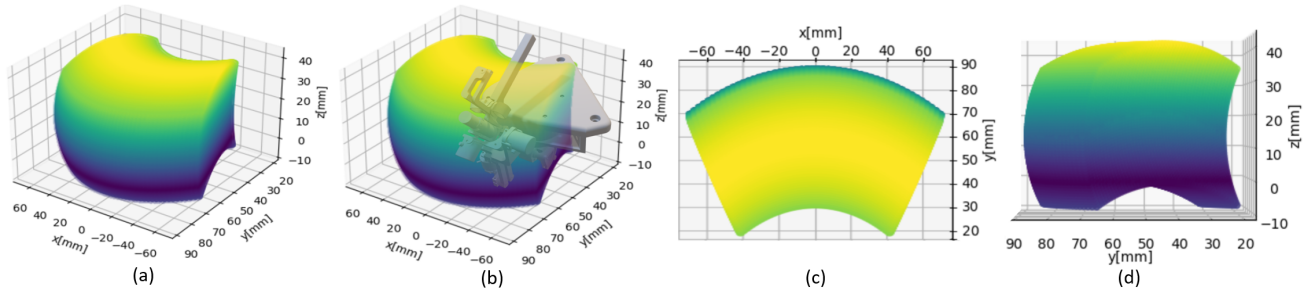

Fig. 5. Controller's workspace from different view points. (a)Isometric view, (b)Isometric view with the controller, (c)top view, and (d)side view are shown.

TABLE I

PARAMETERS FOR THE SIMULATIONS

Experiment	A	B	C	D
Plane	x-y		y-z	
Diameter [mm]	0.5	10.0	0.5	10.0
Width [mm]	0.03	1.0	0.03	1.0

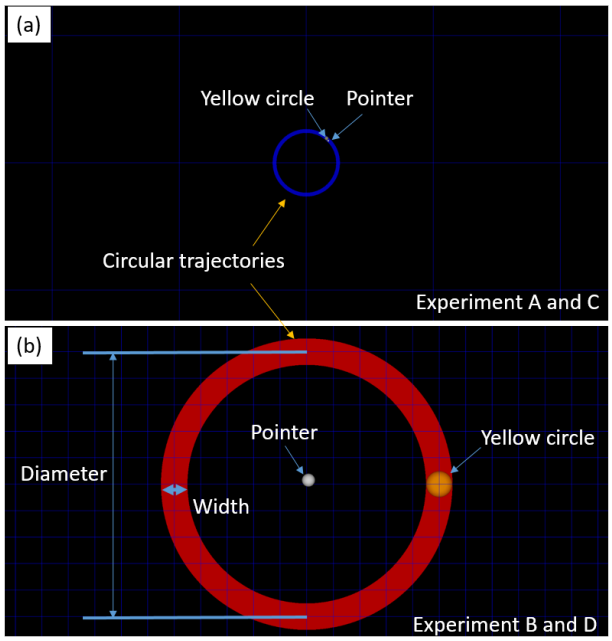

Fig. 6. Screenshots of the trajectory following experiments. (a)The 0.5 mm diameter circle for the experiments A and B, and (b)10.0 mm diameter circle for the experiments B and D. The yellow circle moves counter clockwise as the white pointer touches the yellow circle. The color of ring turns from red to blue when the pointer is within the ring.

same circle appears five times in total for each experiment. The first two circles are assigned as the practice phases and the following three circles are used for data collection. The participants are allowed to have an intermission in between tracing each circle. To align the participants' focus, they were asked to ignore the task completion time and stay inside the ring as much as they can.

The motors on the controller were only used for the gravity compensation. The velocity information passed from the controller to the simulator is integrated, and it is used as the position of the pointer. Since the focus of this work is to investigate the controller's precision with a low scaling factor, the force feedback was disabled and excluded in the experiments. A fixed scaling factor of 3x was used throughout the experiments for all the participants.

B. Results

The 2D position error (distance of the pointer from the middle of the ring's width in the radial direction) and standard deviation (SD) were calculated for each circle at a rate of 1000 Hz. To eliminate the uncertainty caused by lack of the depth perception in the simulation, the components in the depth direction (z-component for the experiments A and B and x-component for the experiments C and D) were disregarded from the computation of the error.

To calculate the 3D positioning accuracy, x- and y-values from the x-y plane experiments and z-values from the y-z plane experiments are used. Then, the mean 3D positioning error and SD for 3 trials were calculated and plotted for each experiment for each participant (Fig. 7). Although the x-y and y-z plane data are collected from the separate experiments, it is assumed that the z-data from the y-z plane experiments represent the accuracy of the z-direction that would be obtained for 3D motion when sufficient depth information is provided. The mean positioning errors for the 0.5 mm circle experiment are within the width of the circle for all the participants. For the 10.0 mm experiments, both the mean positioning errors and SD are inside the circle's width.

As the participants were instructed to stay within the ring rather than to trace the middle of the ring's width, root-mean-squared error (RMSE) or mean absolute error (MAE) do not properly represent the participants' performance. Therefore, the mean error and SD, the deviation of the pointer's position from the average position, are employed as the evaluation criteria of their performance.

IV. DISCUSSIONS

For micro- and supermicrosugery, precisions of 100 μm and 30 μm are required respectively. Although the participants of the experiment were all novice, all of them were able to achieve the precision required for microsurgery. In addition, three out of ten participants were able to exhibit nearly or less than 30 μm precision which is required for

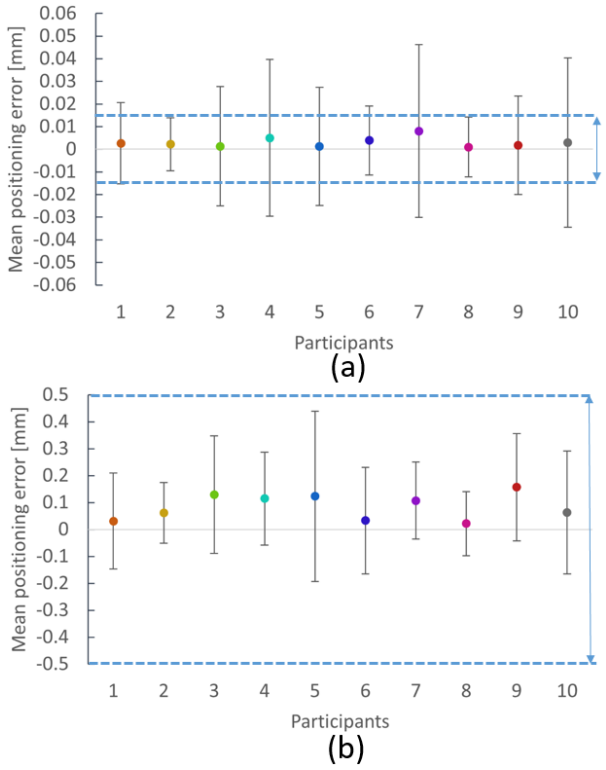

Fig. 7. Mean and SD of the 3D positioning error for (a)0.5 mm circle and (b)10.0 mm circle. The blue dashed lines and arrows indicate the width of the circles.

TABLE II

3D BIDIRECTIONAL PRECISION FOR 0.5 MM CIRCLE EXPERIMENT FOR EACH PARTICIPANT. THE BIDIRECTIONAL PRECISIONS NEARLY OR LESS THAN 0.03 MM, WHICH IS REQUIRED FOR SUPERMICROSURGERY, ARE IN BOLD.

Participant	Bidirectional precision (2SD) [mm]	Participant	Bidirectional precision (2SD) [mm]
1	0.0358	6	**0.0305**
2	**0.0234**	7	0.0763
3	0.0528	8	**0.0265**
4	0.0692	9	0.0436
5	0.0521	10	0.0747

supermicrosurgery (Table II). The results indicate that even lesser skilled microsurgeons, who are not able reach the 30 μm precision, would be able to perform supermicrosurgery by using the presented controller with a 3x scaling factor. Typically, more than twice as large scaling factor is employed for micro- and supermicrosurgery. However, the proposed controller achieves a smaller scaling factor through the method of utilizing the fingertip and wrist motions combined with a handrest. This allows for even the novice participants to reach the level of precision to perform the technically demanding tasks that micro- and supermicrosurgery require.

Since the participants were instructed to ignore the completion time, it is possible that some participants were able to perform better than the others just because they spent

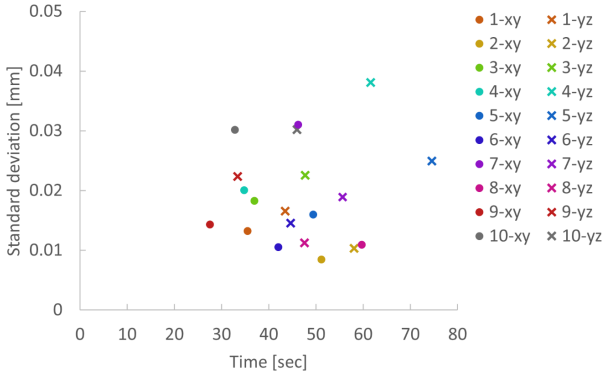

Fig. 8. Task completion time vs. SD for tracing the 0.5 mm circle in x-y and y-z planes (experiment A and C) for each participant. No correlation between the time and SD is observed.

longer time and performed the tasks more carefully. To investigate this, the task completion time and the precision (SD) for the 0.5 mm circle experiments were plotted (Fig. 8). The results indicate there is no notable correlation between the task completion time and the precision for the x-y plane experiment. For the y-z plane experiment, there is a slight trend of increase in the SD as the completion time increases. This trend is reasonable because some participants commented that the y-z plane experiment was more difficult. Hence, the performance seems dependent on the participant's skill rather than the time spent to complete the task.

During the experiments, we observed a tendency of the pointer slipping toward the direction of the lighter joint axis or single joint axis when the motion includes multiple axis components (Fig. 9). This is because the force required to move each joint axis of the controller was different due to the difference in the mechanical impedance. The effect is more observable for the 0.5 mm circle tracing because of the scale of the circle but it will be visible for the 10.0 mm circle tracing as well if the trajectory is zoomed. Since all the linkages of the current prototype are made out of 3D printed parts, manufacturing the parts with metal (i.e. aluminum) with high precision machining will reduce the misalignment of the axis and wobbling. Therefore, the performance of the controller could be better and the achievable precision could be even lower if the mechanism is refined. Moreover, friction or viscosity could be added in the software to achieve more isotropic impedance.

Currently, the prototype has insufficient height and depth workspace. To meet the workspace requirement, the design parameters need to be optimized. For instance, the depth can simply be improved by changing the central angle of the circular sector (indicated in Fig. 4) which is used for gear reduction. If the central angle of the circular sector for θ_2 is modified from the current value of $\pm 27.5^\circ$ to $\pm 70.0^\circ$, the depth requirement can be satisfied. For the height, the linkage length l_{23} should be increased from 45 mm to 80 mm and the central circular sector angle for θ_3 needs to be changed from $\pm 32.5^\circ$ to $\pm 75.0^\circ$. Besides, the yaw, pitch, and roll's range of motion can be increased by implementing smaller encoders

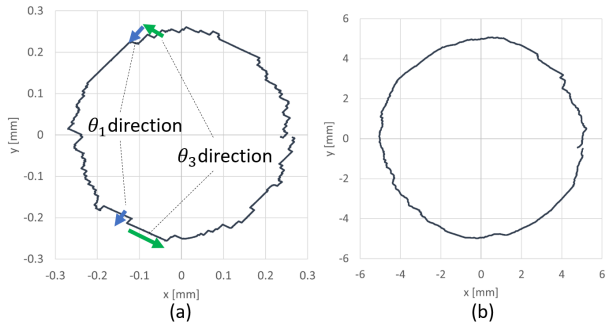

Fig. 9. The pointer trajectories for one participant. The results for (a)experiment A (0.5 mm circle on x-y plane), and (b)experiment C (10.0 mm circle on x-y plane) are shown. The blue arrow indicates the motion in the θ_1 joint axis direction, and the green arrow shows the motion in the θ_3 axis direction. The controller tends to slip in the single joint axis direction because the mechanical impedance is lower along the single joint axis direction.

such that the interferences between the encoders and linkages are avoided. Implementing those modifications would not cause significant impedance or size changes and thus, the controller would still possess the claimed advantages.

The current controller does not provide torque feedback about the yaw, pitch, and roll axis. As adding motors to these axis will increase the weight and inertia, it may be challenging to keep the performance of the controller the same. However, by having dynamic compensation in the software, it could be possible to add the orientational torque feedback while maintaining the manoeuvrability.

V. CONCLUSIONS

This paper presented a new haptic controller that allows the user to perform sub-millimeter as well as centimeter range tasks with a low constant scaling factor using the wrist and fingertip motions targeted for robotically assisted micro- and supermicrosurgery. Because of the unique arrangement of the controller's DOFs around a handrest, the controller achieved to be compact and suitable for robotic microsurgery with a conventional microsurgical setup which cannot be satisfied by the existing haptic controllers. In addition, while the microsurgical controllers do not have the haptic feedback function, the presented controller is equipped with translational and pinching force feedback which is expected to contribute to the improvement of surgical output. To investigate the feasibility of using a single low scaling factor for both fine and large motions by using the fingertip and wrist motions, a simulational study was conducted with a prototype. The results indicated that although the anisotropic mechanical impedance made controlling the pointer challenging, especially for the smaller circles, the participants were able to trace 0.5 mm diameter circles, which represent microsurgery level task, with a bidirectional precision of 0.0234 - 0.0763 mm with a scaling factor of 3x. Furthermore, larger 10.0 mm diameter circles were traceable without changing the scaling factor.

To address the issue of prolonged surgical time for the current robotic microsurgery, we plan to investigate the relationship of the scaling factor and task completion time/achievable accuracy. In other words, the performance of the control based on the fingertip and wrist motion and the control with the arm motion will be compared. Also, the optimal scaling factor for the presented controller will be explored after refining the mechanism.

ACKNOWLEDGMENT

The authors would like to thank the members of Riverfield inc. for their support and contribution throughout the entire project.

REFERENCES

[1] M. Mitsuishi, A. Morita, N. Sugita, S. Sora, R. Mochizuki, K. Tanimoto, Y. M. Baek, H. Takahashi, and K. Harada, "Master–slave robotic platform and its feasibility study for micro-neurosurgery," *The International Journal of Medical Robotics and Computer Assisted Surgery*, vol. 9, no. 2, pp. 180–189, 2013.

[2] R. Cau, F. Schoenmakers, M. Steinbuch, T. van Mulken, and R. R. van der Hulst, "Design and preliminary test results of a novel microsurgical telemanipulator system," in *5th IEEE RAS/EMBS International Conference on Biomedical Robotics and Biomechatronics*. IEEE, 2014, pp. 352–356.

[3] R. Cau, "Design and realization of a master-slave system for reconstructive microsurgery," Ph.D. dissertation, Technische Universiteit Eindhoven, 2014.

[4] T. D. Dobbs, O. Cundy, H. Samarendra, K. Khan, and I. S. Whitaker, "A systematic review of the role of robotics in plastic and reconstructive surgery—from inception to the future," *Frontiers in surgery*, vol. 4, p. 66, 2017.

[5] A. E. Ibrahim, K. A. Sarhane, and J. C. Selber, "New frontiers in robotic-assisted microsurgical reconstruction," *Clinics in Plastic Surgery*, vol. 44, no. 2, pp. 415–423, 2017.

[6] Y. Jonis, J. J. Profar, T. J. van Mulken, and S. Qiu, "The musa robot and its applicability in lymphatic surgery," *Plastic and Aesthetic Research*, vol. 10, no. 29, 2023.

[7] A. Ballestín, G. Malzone, G. Menichini, E. Lucattelli, and M. Innocenti, "New robotic system with wristed microinstruments allows precise reconstructive microsurgery: preclinical study," *Annals of Surgical Oncology*, vol. 29, no. 12, pp. 7859–7867, 2022.

[8] T. J. van Mulken, R. M. Schols, A. M. Scharmga, B. Winkens, R. Cau, F. B. Schoenmakers, S. S. Qiu, R. R. van der Hulst, and M. R. R. G. K. X. H. . L. T. M. . P. A. A. . H. J. E. . D. D. S. . B. J. E. . S. J. . R. M. E. 1, "First-in-human robotic supermicrosurgery using a dedicated microsurgical robot for treating breast cancer-related lymphedema: a randomized pilot trial," *Nature communications*, vol. 11, no. 1, p. 757, 2020.

[9] N. Lindenblatt, L. Grünherz, A. Wang, E. Gousopoulos, C. Barbon, S. Uyulmaz, and P. Giovanoli, "Early experience using a new robotic microsurgical system for lymphatic surgery," *Plastic and Reconstructive Surgery Global Open*, vol. 10, no. 1, 2022.

[10] E. Gousopoulos, L. Grünherz, P. Giovanoli, and N. Lindenblatt, "Robotic-assisted microsurgery for lymphedema treatment," *Plastic and Aesthetic Research*, vol. 10, no. 7, 2023.

[11] S. Jeong and K. Tadano, "Manipulation of a master manipulator with a combined-grip-handle of pinch and power grips," *The International Journal of Medical Robotics and Computer Assisted Surgery*, vol. 16, no. 2, p. e2065, 2020.

[12] P. L. Padilla, J. Shuck, and J. C. Selber, "Robotics in plastic surgery," *Current Surgery Reports*, vol. 11, no. 2, pp. 23–29, 2023.

[13] S. Jeong and K. Tadano, "Force feedback on hand rest function in master manipulator for robotic surgery," in *2021 IEEE/RSJ International Conference on Intelligent Robots and Systems (IROS)*. IEEE, 2021, pp. 1815–1820.

[14] 3D Systems Inc., "Haptic devices," https://www.3dsystems.com/scanners-haptics, accessed: 2023-08-25.

[15] Force Dimension, https://www.forcedimension.com, accessed: 2023-08-25.